

Utilizing polypropylene fibers to improve physical and mechanical properties of concrete

Textile Research Journal
00(00) 1–9
© The Author(s) 2011
Reprints and permissions:
sagepub.co.uk/journalsPermissions.nav
DOI: 10.1177/0040517511420767
trj.sagepub.com



Roohollah Bagherzadeh^{1,2}, Abdol-Hossein Sadeghi¹ and Masoud Latifi¹

Abstract

The influence of polypropylene fibers has been studied in different proportioning and fiber aspect ratios to improve physical and mechanical properties of fiber-reinforced concretes. Fibers are used in two different lengths (12 mm and 19 mm) and proportions (0.1% and 0.3%) in concrete mixture design. Hardened concrete properties, such as 7- and 28-day compressive strength, splitting tensile strength, flexural strength, water and air absorption, and restrained shrinkage cracking were evaluated.

No statistically significant effects were observed for polypropylene fibers on the compressive strength of concrete, while toughness indexes, splitting tensile and flexural strength and durability parameters showed an increase in the presence of polypropylene fibers. Increased fiber availability (fiber aspect ratio) in the concrete matrix, in addition to the ability of longer polypropylene fibers to bridge on the micro cracks, are suggested as the reasons for the enhancement in mechanical properties. Finally, crack width in fiber-reinforced concrete is calculated analytically with fiber property variables (fiber type, length, diameter and proportion). Results are compared with experimental values and concluded that with an increase in fiber length and/or decrease in fiber diameter crack width, decrease significantly.

Keywords

Fiber-reinforced concrete, polypropylene fiber, mechanical properties

Introduction

Concrete is widely used in structural engineering with its high compressive strength, low-cost and abundant raw material. But common concrete has some shortcomings, for example, shrinkage and cracking, low tensile and flexural strength, poor toughness, high brittleness, low shock resistance and so on, that restrict its applications. It is well documented^{1–4} that the cracks generally develop due to following reasons:

- plastic shrinkage: due to the loss of water, in the plastic state, from evaporation.
- autogenous shrinkage: chemical shrinkage (lower volume of hydrates than cement and water) + auto-dessiccation (reduction in the pore water due to hydration)
- thermal contraction (or thermal shrinkage): due to the decrease in temperature after setting
- drying shrinkage: due to the loss of water to the environment in the hardened state

- carbonation shrinkage: volume reduction due to the reaction of hydrated cement paste with CO₂ in the presence of moisture.

To counteract the cracks, a fighting strategy has come into use in the recent years, which mixes the concrete with discrete fibers.¹ Fiber-reinforced concrete (FRC) has been successfully used in construction with its excellent flexural-tensile strength, resistance to splitting, impact resistance and excellent permeability, and frost

¹ATMT Research Institute, Textile Engineering Department, Amirkabir University of Technology, Tehran, Iran.

²Centre for Material and Fibre Innovation, ITRI, Deakin University, Waurn Ponds, VIC 3217, Australia.

Corresponding author:

Masoud Latifi, ATMT Research Institute, Textile Engineering Department, Amirkabir University of Technology, Tehran, Iran
Email: latifi@aut.ac.ir

resistance. It is also an effective way to increase toughness, shock resistance, and resistance to plastic shrinkage cracking of the mortar.^{1,5}

Several different types of fibers, both manmade and natural, have been incorporated into concrete. Use of natural fibers in concrete precedes the advent of conventional reinforced concrete in the historical context.⁶⁻⁸ However, the technical aspects of FRC systems remained essentially undeveloped. Since the advent of fiber reinforcing of concrete in the 1940s, a great deal of testing has been conducted on the various fibrous materials to determine the actual characteristics and advantages for each product.

FRC properties, such as crack resistance, reinforcement and increase in toughness are dependent on the mechanical properties of the fiber, bonding properties of the fiber and matrix, as well as the quantity and distribution within the matrix of the fibers.⁹⁻¹¹ In relation to the elastic modulus, fibers are divided into two types, those that the elastic modulus of fibers is less than the elastic modulus of the matrix: i.e. cellulose fiber, polypropylene (PP) fiber, polyacrylonitrile (PAN) fiber, etc., and those that the elastic modulus of fibers is greater than the elastic modulus of the matrix: i.e. asbestos fibers, glass fiber, steel fiber, carbon fiber, aramid fiber, etc. Many tests have been made to study the feasibility of adding fibers and their advantages to concrete as an additive. Low modulus fibers primarily control the propagation of cracks and limit the crack width. To reduce the phenomenon of shrinkage and the induced cracking, satisfactory results are obtained by adding a combination of low and high modulus fibers.¹² Alhozaimy et al.⁹ observed that an additional amount of 0.1% PP fibers in the plain concrete had a 44% increase in flexural toughness of the concrete. Hughes and Fattuhi¹³ suggest that compressive strength decreases but flexural properties are improved with increasing fiber content. It is also reported⁴ that the compressive and splitting tensile strengths and modulus of rupture (MOR) of the nylon FRC improved by 6.3%, 6.7%, and 4.3%, respectively, over those of the PP fiber-reinforced concrete. On the other hand, some

researchers^{2,14} have reported that the PP fibers have excellent alkali resistance in comparing with other polymeric fibers like nylon and acrylic fibers. Pakravan et al.³ also reported no changes in strength of PP fibers after soaking in alkali for periods of 28 and 56 days. Good alkali resistance of PP fibers makes them a more suitable option for using in cement composites in an alkali environment.

The performance of fibers as reinforcement in cement-based materials for different fibers (glass, PP, PAN, and high strength nylon 66) by investigation of bonding characteristic of fiber to cement matrix has been carried out by Pakravan et al.³ It was concluded that PP fibers, in spite of their hydrophobic nature and weak wetting by cement paste, showed better bonding than others.

There are well-documented reports in the area of adding fibers in concrete, however, there is still a lack of studies on the best volume fractions of fibers in the concrete mixture. This study presents comprehensive experimental data and a theoretical approach regarding the effects of adding PP fibers with different fiber lengths and diameter, and different volume fractions, on the physical and mechanical properties of FRC.

Materials and methods

Materials

PP fibers used in this study were provided by the PP fiber Production Company. Specification of the fibers employed in this study are presented in Table 1. Ordinary Portland cement conforming to IS 12269 was used for the concrete mixtures. River sand with a specific gravity of 2.65 (g/cm³) and fineness modulus of 2.64 (g/cm³) was used as the fine aggregate.

Mixing and curing

Trial mixtures were prepared to obtain a target strength of 40 MPa at 28 days, along with a good workability.

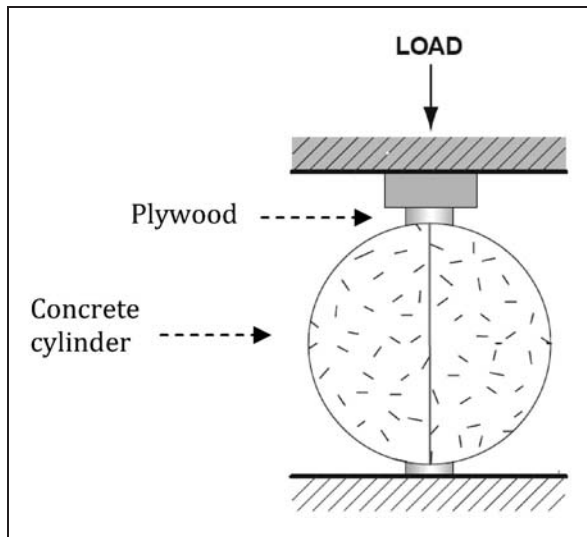
Table 1. Physical and mechanical properties of the various fibers used

Code	Length (mm)	Type	Diameter (mm)	Aspect ratio*	Specific gravity	Tensile strength (MPa)	Elastic modulus (GPa)	Failure strain (%)
F1	12	Monofilament	0.22	54.54	0.91	445	5.0	18
F2	19	Monofilament	0.22	86.36	0.91	450	5.0	18
F3	12	Monofilament	0.46	26	0.91	480	5.5	19
F4	12	Fibrillate	75 (equivalent diameter)	0.16	0.91	450	5.0	16

*length divided per diameter.

Table 2. Concrete mixture proportions used in the study

Sample code	Type	Fiber
		Volume fraction % (per 1 m ³)
P0	-	-
P1	F1	0.1
P2	F2	0.1
P3	F3	0.3
P4	F4	0.3

**Figure 1.** Schematic of split tensile strength test.

The final mixture design used in this study was composed of 350 kg/m³ cement, 184 kg/m³ water, 0.40 water/cement percentage (W/C), and 1.35% naphthalene-based superplasticizer (supplied from LanYa Concrete Admixtures Co.). The total dosage of fibers was maintained at 0.1–0.3%, primarily from the point of view of providing good workability and no balling of fibers during mixing (Table 2).

The sand, cement, and other additive were first mixed dry in a pan mixer with a capacity of 100 kg for a period of 2 min. The naphthalene-based superplasticizer was then mixed thoroughly with the mixing water and added to the mixer. First, fibers were dispersed by hand and then were mixed in the mixture for a total time of 4 min to achieve a uniform distribution throughout the concrete, which was mixed.

Fresh concrete was cast in steel molds and compacted on a vibrating table. For the curing function, the specimens were kept covered in their molds for 24 h. The FRC specimens had less bleeding than the control

concrete specimen. After demolding, concrete specimens were placed in 20±2 °C water for 28 days for curing. They were removed from water and placed in the laboratory environment for 2 h before carrying out the tests. All tests were performed according to relevant standards.

Physical and mechanical tests

Compressive strength. A universal testing machine with a capacity of 100 tonnes was used for testing the compressive strengths of nine 150×150×150 mm specimens. Cube specimens at 7, and 28 days from casting were tested at a loading rate of 14 N/mm²/min according to ASTM C39. The compressive strength was interpreted as the stress generated from the result of compression load per area of specimen surface. The results for each specimen are based on an average value of three replicate specimens.

Flexural strength. Flexural strength at 28 days of curing test was conducted according to the requirements of ASTM C 1609 using three 100×100×500 mm beams under third-point loading on a simply supported span of 400 mm. According to ASTM standards, the results of the flexural strength test are interpreted by calculating flexural stress as follows:

$$R = \frac{PL}{bd^2} \quad (1)$$

where R is the flexural strength (modulus of rupture), P is the maximum indicated load, L is the span length, b is the width of the specimen, and d is the depth of the specimen.

Tensile strength. Split (Brazilian) tensile strength at 28 days of curing test of three 150×300 mm cylinders is an indirect measurement of tensile strength of the concrete that was conducted according to the requirements of ASTM C496. In the split tensile strength test, a cylindrical concrete specimen was placed on diametrical compressive force along the length of the specimen (Figure 1). The load was applied continuously at a constant rate until the failure of cylinder along the vertical diameter. To allow the uniform distribution of applied compressive load, strips of plywood are placed between the specimen and loading plates of the testing machine.

Splitting tensile strength of a specimen can be evaluated from equation 2:

$$T = \frac{2P}{\pi ld} \quad (2)$$

where T is the tensile strength, P is the compression load at failure, l is the length of the cylinder, and d is the diameter of the cylinder.

Air and water permeability. Water absorption at 28 days of curing tests of three $100 \times 100 \times 100$ mm concrete beams was conducted according to the requirements of ASTM C1585.

Air (oxygen gas) permeability at 28 days of curing test of three 150×300 mm cylinders was performed for each specimen according to the recommendation of TC 116-PCD.

Shrinkage cracking. For determining the effect of adding fiber to the crack forming in concrete, tests have been carried out using narrow rings of concrete next to rigid steel rings according to the method that was used in previous research works.¹⁵⁻¹⁷ An original process made it possible to measure the crack widths and to follow the development of cracking. A video camera continuously filmed the crack created at different levels (top, middle and bottom). Observations begin at the birth of the crack and continue until the end of the test (approx. 4 weeks). Images have a size of $15 \text{ mm} \times 15 \text{ mm}$. They are developed with an image analysis process. The image is divided into 512×512 pixels. After image analysis, values of changes in sample length and width were measured (Table 4). One pixel corresponds to 0.0293 mm , so the crack widths can already be seen at 0.03 mm . The dimensions of the sample and the measurement setup are shown in Figure 2.

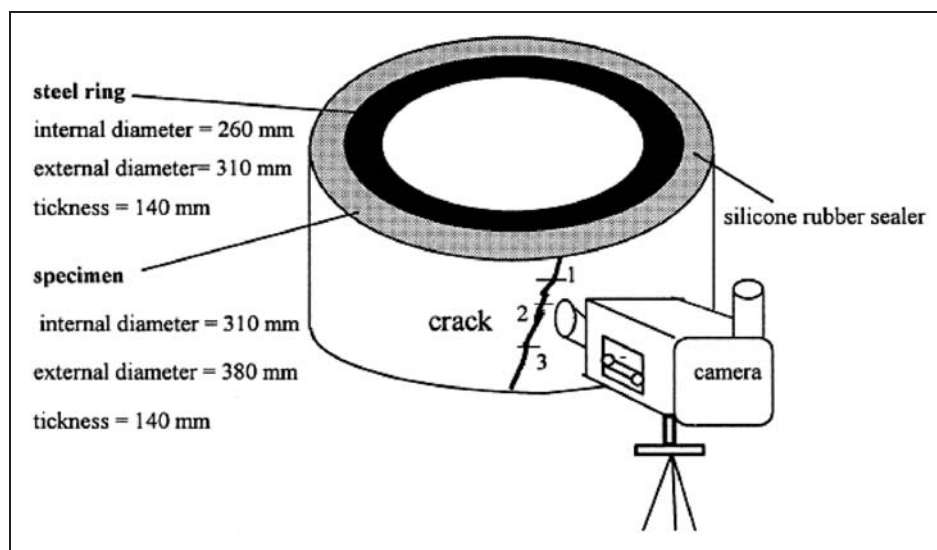


Figure 2. Test setup to measure crack width using image analysis and dimensions of the ring specimen.

Contribution of polypropylene fibers in crack reduction

Shrinkage cracking is a major concern for concrete structures, especially for flat structures, such as highway pavement, slabs and walls. The behavior of FRC under loading can be understood from Figure 3. The plain concrete structure cracks into two pieces when the structure is subjected to the peak tensile load and cannot withstand further load or deformation.⁵ The FRC structure cracks at the same peak tensile load, but does not separate and can maintain a load to very large deformations. The area under the curve shows the energy absorbed by the FRCs when subjected to tensile load. This can be termed as the post cracking response of the FRCs. The real advantage of adding fibers is when fibers bridge these cracks and undergo pull-out processes, such that the deformation can

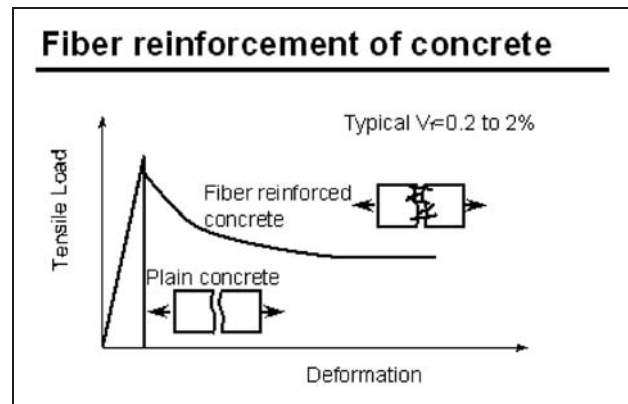


Figure 3. Tensile load versus deformation for plain and FRC.

continue only with the further input of energy from the loading source.

Theoretical discussion for prediction of restrained concrete crack width

Grzybowski and Shah¹⁸ have developed a theoretical model to predict the cracking response of FRC subjected to restrained shrinkage. This model can generally be applied to three-dimensional structures subjected to a given drying environment with a specified boundary restraint. It is used to predict the number and the widths of cracks in a structure submitted to a restrained shrinkage (tunnels, bridges, slabs, etc.). The effects of the size and the form of the structure are included in this model.

The physical concept of the development of cracks under restrained conditions can be described as follows. At a given time, when the shrinkage is restrained, a tensile stress develops. It depends on the strain and the elastic modulus of the composite, $E(t)$, at time t . It can be expressed as follows:

$$\sigma(t) = E(t)\varepsilon_{sh}(t) - \sigma^R(t) \quad (3)$$

where $\sigma^R(t)$ is the stress reduction induced by relaxation effects.¹⁹

In this study, the increment of time is equal to 0.5 days, corresponding to the measurement of free shrinkage. Admittedly, the ring sample is subjected only to radial drying and the circumference of the ring remains constant because of the restraint. As a consequence of the imposed strain, stresses are introduced into the sample. A non-linear stress-strain curve was assumed to represent the uniaxial tensile behavior of concrete (damage theory). It is important to include the change in strength and stiffness with time:¹⁸

$$E_c(t) = E_{c28} \sqrt{\frac{f_c(t)}{f_{c28}}} \text{ and } f_c(t) = \frac{t}{4 + 0.85t} f_{c28} \quad (4)$$

The stress due to shrinkage is partially reduced by relaxation. The reduction in stress can be computed using relaxation curves available in many writings.²⁰ With time, tensile stress increases. A crack forms when this stress exceeds the tensile strength of the composite. After cracking, the shrinkage process continues. The stress developed in the sample depends on the force transferred across the crack (cohesion and bond). For FRC, the tensile stresses across the crack are much higher. That depends on the content and the geometry of the fibers. The criterion stress, crack width is given by the relationship proposed by Malmberg²¹ determined

from a pull-out test:

$$P = p \frac{1}{2} \tau_v \left[\frac{w}{w_s} - \left(\frac{w}{w_s} \right)^2 + \frac{1}{2} \alpha \left(\frac{w}{w_s} \right)^2 + K' \frac{w}{w_s} \right] \quad (5)$$

where w_s is the maximum crack width when all the fibers begin to slip:

$$w_s = \frac{\tau V_f^2}{d E_f} \text{ if } \alpha + K' \leq 1 \quad (6)$$

$$w_s = \frac{\tau V_f^2}{d E_f} (\alpha + K') \text{ if } \alpha + K' > 1 \quad (7)$$

Stress per unit of surface is equal to: $\sigma = N \times p$; where N is the number of fibers per unit of surface: $N = (8V_f)/(\pi^2 d^2)$ for cylindrical fibers; p is the perimeter of the fiber; l the length of the fiber; d the diameter of the fiber; V_f the volume of fibers; W is the crack width; W_s the width of critical crack; τ_v is the interfacial shear strength; τ_g the frictional shear strength; and K' is the anchorage force on the end of the fiber. The interfacial shear τ_v (τ_{\max}) can be determined from the equation proposed by Debicki.²² The stress is obtained from the equilibrium equation of an anchored fiber of length l_c :

$$\tau_{\max} = \frac{2S\sigma_{f\max}}{pl_c} \quad (8)$$

where S is the cross-section area of the fiber; τ_{\max} the ultimate fiber strength (600 MPa for PP fibers); and p is the perimeter of a straight section of fiber. The interfacial shear τ_v is estimated from the results of bending tests on notched prisms after the peak, by supposing that fibers alone support the load (for fiber code F1 obtained around 1.70 GPa). It is assumed that fibers have a circular cross-section (as can be seen from Figure 4), so we have:

$$S = \frac{\pi d^2}{4} \quad (9)$$

$$den = \frac{\rho S}{1000} \times 9 \quad (10)$$

where den is denier of the fiber used (g/9000 m), ρ is density of fiber (g/cm³), and d is diameter of fiber in micron. From equation (7), (8), (9), and (10), it is easy to predict the maximum crack width in the FRC.

Results and discussion

Physical and mechanical properties

Physical and mechanical properties of all samples are tabulated in Table 3. Each of the results is the average

value of three test specimens, and for each test, the values were statistically analyzed by the ANOVA technique using SPSS software V12 at a 0.95 level of confidence.

Following the results of compression strength in Table 3, it can be concluded that fibers added to the concrete specimens have no significant influence on 7 and 28 day compressive strength of specimens. Although, it is reported that using fibers in concrete have more efficient effect on further loading after collapse.⁵

Flexural strength results of specimens (Table 3) compared to control concrete without fibers (P0), showed an appreciable increase in flexural strength. Also, increase in the fiber volume fraction clearly shows the better performance. Among all FRCs, specimens containing a higher proportion of fiber (P3 and P4), showed the

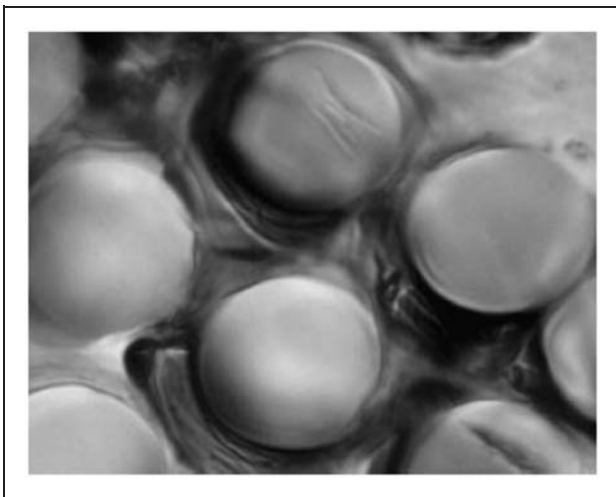


Figure 4. Cross-section of PP fibers.

maximum flexural strength. This is due to the contribution of more fibers during tensile load before fracture of the samples. Also it can be observed that the specimen with fibrillated PP fiber showed better flexural strength in comparison with specimens with monofilament fibers. The reason could be due to less slipping properties of the fibrillated PP fibers used in the P4 specimen, which gives high reinforcement and connectivity index in compression with monofilament fibers that otherwise could be slipped easily after continuing the load (Figure 5).

Split tensile strengths of PP fiber concretes (Table 3) were found to be higher compared to reference concrete. The splitting tensile strengths of the P2 and P3 were

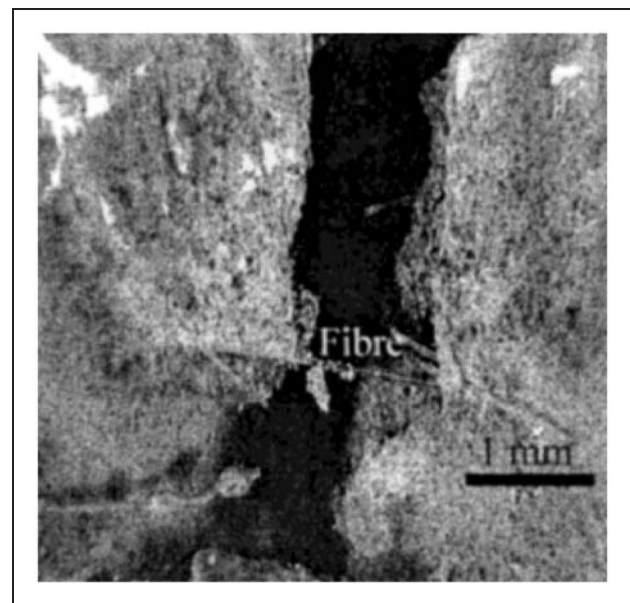


Figure 5. Slipping of the monofilament PP fiber during the flexural strength test.

Table 3. Results of physical and mechanical properties of specimens

Specimens code	P0	P1	P2	P3	P4
Strength (MPa)					
Compression (7 days)	39.4	42.3	41.7	38.4	39.2
Compression (28 days)	49.0	51.8	51.6	49.3	50.1
Splitting tensile	9.5	9.8	10.2	11.0	10.8
Flexural	8.7	9.2	8.9	9.7	10.2
Bending toughness (kg.m)					
toughness index I_5	–	1.29	1.28	1.25	1.28
toughness index I_{10}	–	–	1.52	1.47	1.03
toughness index I_{30}	–	–	–	1.68	–
Water infusion (mm)	14.2	14	13.5	13.4	14.03
Air permeability (m^2)	6.68	6.60	6.52	6.48	6.63

Toughness indexes I_5 , I_{10} and I_{30} are calculated as ratios of the area of the load-deflection curve up to 3, 5.5 and 15.5 times the first-crack deflection divided by the area of the load-deflection curve up to the first-crack deflection, respectively (according to ASTM C 1018).

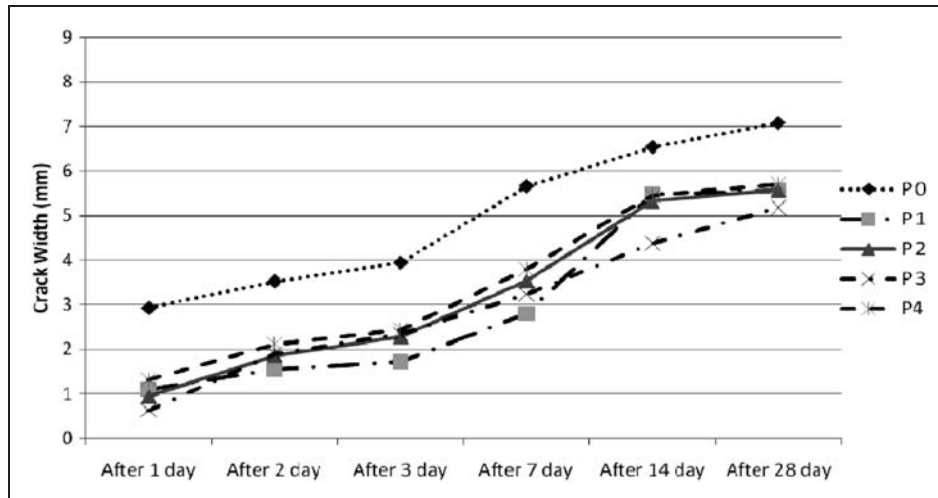


Figure 6. Rate of changes in sample crack width (mm).

7.36% and 15.79% higher, respectively, than that of the unreinforced control concrete (P0) which show the good improvement in comparison with the results of Song et al.⁴ It can also be observed that specimens containing the PP fiber with higher aspect ratio or high volume fraction (P2 and P3) show the better split tensile strength among all concretes. Enhancement in split tensile strength is expected when the fiber proportion is increased since the plane of failure is well defined (diametric). The higher the number of fibers bridging on the diametrical 'splitting' crack, the higher would be the split tensile strength. Short length and fibrillated fiber-reinforced specimens (P1 and P4), possibly owing to their short fiber lengths or less amount of aspect ratio, did not perform as well as the other two samples.

Toughness is based on the total energy absorbed prior to compete failure. The main properties influencing toughness and maximum loading of FRC are based on the type of fibers used, volume percent of the fiber, the aspect ratio and the orientation of the fibers in the matrix.^{1-3,10} Bending toughness results of the sample (area under curve of load-displacement) are shown in Table 3. It can be concluded that using PP fiber in concrete has a significant effect on toughness and its indexes as shown in Table 3. Furthermore with the increase in fiber length and dosage, energy absorption and toughness indexes improved. So, crack width should decrease as a result of energy absorption improvement.

By adding the fiber to concrete, durability parameters (water and air permeability) of concrete were improved as is shown in Table 3. It is clearly shown that introducing fibers to the concrete have a direct effect on the water and air infusion behavior of concrete. The water infusion and air permeability of all specimens decreases by adding monofilament PP fibers although the fiber aspect ratio and dosage have no significant effect on the

Table 4. Maximum crack width and total crack area of different samples

Sample code	Maximum crack width (mm)	Predicted maximum crack width (mm)	Crack area (mm ²)
P0	3.2	-	430
P1	2.1	2.07	295
P2	2.0	2.11	310
P3	1.8	1.77	285
P4	2.3	2.41	328

durability parameter of specimens. Fibrillated PP fibers have no statistically significant effect on air and water permeability of specimens.

Effect of fiber aspect ratio on crack control

By adding PP fibers to the cement matrix, free shrinkage decreases. This decrease is very large especially at the early stage of casting, as shown in Figure 6. When a crack is formed in FRC, fibers that bridge the crack prevent it from opening more. With the action of shrinkage, fibers transmit forces through the crack and thus create tensile stresses along the ring. If loads transmitted by fibers are very small, as for composites containing very low volumes of fibers, then the second crack will not form because the tensile stress transmitted across the crack is smaller than the tensile strength of the matrix. When the fiber proportioning is increased, more cracks with a smaller width develop. Experimental results confirm this tendency. The evolution of cracking with time issued from image analysis for samples, clearly showed that the widest crack width and the total crack width decrease when fibers are added to specimens (Table 4).

As it mentioned in the literature review, one of the more important properties of the concrete fiber is aspect ratio. It is well documented that fibers in concrete have a bridge effect and are very sensitive to size of the material used in mixed design. In Table 4, in the case of P1 and P2, it can be concluded that with increase in fiber length and/or decrease in fiber diameter crack width, the aspect ratio of the fibers (Table 1) decreases significantly for both theoretical and experimental results. This due to the fact that with an increase in aspect ratio of fibers, the specific area of the fibers increases and consequently mechanical entanglement fibers in the concrete increased. Also by comparing the result of crack width of P3 with both P1 and P2, it can be inferred from Table 4 that by increasing the volume fraction of the fiber in the concrete mixture, crack width decreases, which could be affected by a greater 'fiber bridge effect' in the concrete matrix. Finally, monofilament fibers were more effective in controlling shrinkage cracking than their comparable fibrillated counterparts.

Conclusion

The addition of a low volume fraction (0.1–0.3%) of PP fibers is helpful to improve the microstructure and restrain the formation and growth of micro cracks in concrete. Moreover, the continuity and integrity of concrete will be improved and the long-term tensile strength will be developed, which is beneficial to the safety and durability of concrete structures. This study also shows that the aspect ratio of the fiber is an important parameter of fiber reinforcing concrete. Fiber with a higher aspect ratio shows a better improvement in controlling the micro cracks in concrete microstructure. The best aspect ratio without any inference in workability of concrete and bailing of fiber in concrete structure was 86.36 which could be achieved by fiber with a diameter of 22 μ and a length of 19 mm. Also it could be possible to predict the maximum crack width in the FRC through the theoretical method developed in this study by having fiber parameters.

Funding

This research received no specific grant from any funding agency in the public, commercial, or not-for-profit sectors.

Acknowledgements

The authors wish to express their gratitude to Bonyad PP. Fiber Production Co. for providing fiber samples and experimental facility.

References

1. ACI-Committee-544. *State-of-the-art report on fiber reinforced concrete*. Michigan: Farmington Hills, 1996.

2. Brandt AM. *Cement-based composites: Materials, mechanical properties and performance*. Taylor & Francis: Abingdon, 2009.
3. Pakravan HR, Jamshidi M and Latifi M. Performance of fibers embedded in a cementitious matrix. *J Appl Polym Sci* 2010; 116: 1247–1253.
4. Song PS, Hwang S and Sheu BC. Strength properties of nylon- and polypropylene-fiber-reinforced concretes. *Cement Concrete Res* 2005; 35: 1546–1550.
5. Brown R, Shukla A and Natarajan KR. *Fiber reinforcement of concrete structures*. Kingston: University of Rhode Island Transportation Center, 2002.
6. Kalifa P, Chéné G and Gallé C. High-temperature behaviour of HPC with polypropylene fibres: From spalling to microstructure. *Cement Concrete Res* 2001; 31: 1487–1499.
7. Poon CS, Shui ZH and Lam L. Compressive behavior of fiber reinforced high-performance concrete subjected to elevated temperatures. *Cement Concrete Res* 2004; 34: 2215–2222.
8. Suhaendi SL and Horiguchi T. Effect of short fibers on residual permeability and mechanical properties of hybrid fibre reinforced high strength concrete after heat exposition. *Cement Concrete Res* 2006; 36: 1672–1678.
9. Alhozaimy AM, Soroushian P and Mirza F. Mechanical properties of polypropylene fiber reinforced concrete and the effects of pozzolanic materials. *Cement Concrete Composites* 1996; 18: 85–92.
10. Kim DJ, Naaman AE and El-Tawil S. Comparative flexural behavior of four fiber reinforced cementitious composites. *Cement Concrete Composites* 2008; 30: 917–928.
11. Mindess S and Vondran G. Properties of concrete reinforced with fibrillated polypropylene fibres under impact loading. *Cement Concrete Res* 1988; 18: 109–115.
12. Qian CX and Stroeven P. Development of hybrid polypropylene-steel fibre-reinforced concrete. *Cement Concrete Res* 2000; 30: 63–69.
13. Hughes BP and Fattuhi NI. Improving the toughness of high strength cement paste with fibre reinforcement. *Composites* 1976; 7: 185–188.
14. Balaguru P and Slattum K. Test methods for durability of polymeric fibers in concrete and UV light exposure. *Am Concrete Inst, Special Publication* 1995; 155: 115–136.
15. Akkaya Y, Ouyang C and Shah SP. Effect of supplementary cementitious materials on shrinkage and crack development in concrete. *Cement Concrete Composites* 2007; 29: 117–123.
16. Banthia N and Gupta R. Influence of polypropylene fiber geometry on plastic shrinkage cracking in concrete. *Cement Concrete Res* 2006; 36: 1263–1267.
17. Mesbah HA and Buyle-Bodin F. Efficiency of polypropylene and metallic fibres on control of shrinkage and cracking of recycled aggregate mortars. *Construction Building Materials* 1999; 13: 439–447.
18. Grzybowski M and Shah SP. Model to predict cracking in fibre reinforced concrete due to restrained shrinkage. *Magazine Concrete Res* 1989; 41: 125–135.
19. Yao W and Wu K. Study of mechanical properties on polypropylene fiber reinforced concrete. *3rd Asian Symposium on Polymers in Concrete*. Shanghai, China: Tongji University Press, 2000.

20. Bažant ZP. Errata to the paper 'Input of creep and shrinkage characteristics for a structural analysis program'. *Matériaux et Constructions* 1983; 16: 229.
21. Malmberg B and Skarendhal A. Method of studding the cracking of fiber concrete under restrained shrinkage. In: Swamy RN (ed.) *RILEM Symposium on Testing and Test Methods of Fiber Cement Composites*. 1978, pp. 173–179, Construction Press.
22. Debicki G. Mechanical properties of date palm fibres and reinforced date palm fibre concrete in hot-dry climate", Thesis statement, Lyon, INSA, 1988.